J Mater Sci (2012) 47:4187–4193
DOI 10.1007/s10853-012-6273-x

CdS-sensitized ZnO nanorod arrays coated with TiO_2 layer for visible light photoelectrocatalysis

Jianglin Ouyang · Menglei Chang · Xinjun Li

Received: 30 August 2011 / Accepted: 12 January 2012 / Published online: 24 January 2012

Abstract A novel ZnO/CdS/TiO_2 nanorod array composite structure was fabricated by depositing CdS-sensitized layer onto ZnO nanorod arrays via chemical bathing deposition and subsequently coated by TiO_2 protection layer via a vacuum dip-coating process. The films were characterized by x-ray diffraction, field emission scanning electron microscopy, energy dispersive spectrum, and UV–Vis diffuse reflectance spectroscopy. For the films severed as the photoanodes, linear sweep voltammetry and transient photocurrent (i_{ph}) were investigated in a three-electrode system. The photoelectrocatalytic activity was evaluated by the degradation of methylene blue (MB) under visible light irradiation. The results show that the oriented ZnO nanorods are adhered by relatively uniform CdS-sensitized layer and coated with TiO_2 layer. Both the coated and uncoated CdS-sensitized ZnO nanorod arrays exhibit the visible light response and the photoelectrocatalytic activity on the degradation of MB under visible light irradiation. The ZnO/CdS/TiO_2 nanorod array film possesses stable and superior photoelectrocatalytic performance owing to the TiO_2 thin layer protecting the CdS from photocorrosion.

Introduction

Heterogeneous photocatalysis is an advanced oxidation process (AOP), which can degrade a great variety of organic compounds [1]. Titanium dioxide (TiO_2) has been proven as one of the most promising candidates due to its high oxidation efficiency, outstanding chemical stability, and environmentally friendly nature [2–6]. However, the relatively wide band gap of 3.2 eV limits further application of TiO_2 in the visible light region. It is of great interest to develop new photocatalyst to extend the absorption wavelength range into the visible light region. One of the approaches is to introduce the composite system by incorporating a narrow band gap semiconductor (such as CdS [7–9], PbS [10], CdSe [11], and CdTe [12]) serving as the sensitizer. The system, for example TiO_2/CdS [12–15], TiO_2/PbS [16], TiO_2/CdSe [17], and TiO_2/ZnO [18–22], has been reported in the quantum-dot-sensitized solar cells and photocatalytic splitting of water. A growing attention has been drawn to the expansive application on environmental purification. Robert et al. used a coupled CdS/TiO_2 semiconductors suspension for the degradation of Acid Orange II under UV–Vis and visible ($\lambda > 400$ nm) illumination [23]. Ho et al. employed coupled CdSe/TiO_2 for the degradation of 4-chlorophenol (4-CP) in water under the visible light emitted from a 300 W tungsten halogen lamp with a 400 nm cutoff filter [24]. Liao et al. employed nanosized TiO_2/ZnO composite catalyst for the degradation of methyl orange [25]. There are few references on the utilization of CdS/ZnO photocatalyst system for environmental purification under visible light irradiation.

Although the coupling of ZnO with CdS was found to have high conversion efficiency in the quantum-dot-sensitized solar cells, CdS suffers from the drawback of photocorrosion, which is a major obstacle to its potential use in photocatalysis. Recently, a new attempt has been made to prevent CdS nanoparticles from photocorrosion by building a layer of ZnO nanorods on the TiO_2 nanotube/CdS surface for photoelectrocatalytic degradation methyl orange [26].

J. Ouyang · M. Chang · X. Li (✉)
Guangzhou Institute of Energy Conversion, Chinese Academy of Sciences, Guangzhou 510640, People's Republic of China
e-mail: lixj@ms.giec.ac.cn

J. Ouyang · M. Chang
Graduate University of Chinese Academy of Sciences, Beijing 100049, People's Republic of China

Inspiringly, this means could promote the progress of the above sulfur group semiconductors sensitized ZnO in visible light photocatalysis.

Owing to the unidirectional electric channel for the photogenerated electron transport and large internal surface area [27], ZnO nanorod array film is a good candidate for photoelectrochemical (PEC) cells electrode. Herein, a new attempt has been made to construct a ZnO/CdS/TiO_2 nanorod photocatalyst, by depositing CdS-sensitized layer onto ZnO nanorod arrays via chemical bathing deposition and subsequently coated by TiO_2 protection layer via a vacuum dip-coating process. The role of TiO_2 layer to prevent CdS from photocorrosion was evaluated and the photoelectrocatalytic performance on the degradation of methylene blue (MB) under visible light illustration was investigated.

Experimental

Material synthesis

All reagents are of analytical grade and used without any further purification. Conductive F-doped SnO_2 (FTO) glass was purchased from Shenzhen City Xuguang Titanium Co., LTD. Zinc acetate dehydrate ($Zn(CH_3COO)_2{\cdot}2H_2O$), cadmium nitrate ($Cd(NO_3)_2$), thioacetamide ($C_2H_5NS$), and anhydrous ethanol (CH_3CH_2OH) were obtained from Guangzhou Chemical Reagent Factory. Zinc nitrate hydrate ($Zn(NO_3)_2{\cdot}4H_2O$), hexamethylenetetramine ($(CH_2)_6N_4$), sodium nitrate ($NaNO_3$), tetrabutyl orthotitanate ($C_{16}H_{36}O_4Ti$), and diethanolamine ($C_4H_{11}NO_2$) were purchased from Guangdong Guanghua Chemical Factory Co., LTD.

The fabrication of the ZnO/CdS/TiO_2 nanorod array film was carried out by a three-step process: wet-chemical route for synthesizing the ZnO nanorod array film, chemistry bathing deposition (CBD) of CdS on the ZnO nanorod arrays and building a TiO_2 layer by vacuum dip-coating process. The illustration of the typical fabrication of ZnO/CdS/TiO_2 nanorod array film process is shown in Fig. 1.

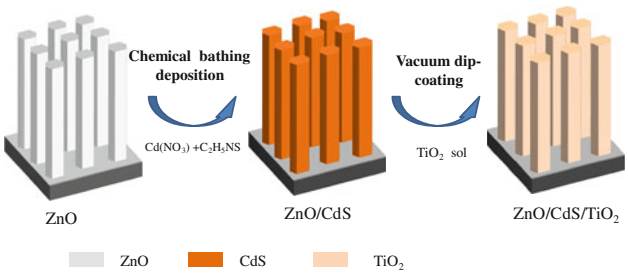

Fig. 1 Schematic illustration for the construction of ZnO/CdS/TiO_2 on the FTO glass

Preparation of seed-coated substrates

Firstly, ZnO seed layer films were deposited on conductive F-doped SnO_2 glass substrates via sol–gel method [28]. In brief, zinc acetate dehydrate ($Zn(CH_3COO)_2{\cdot}2H_2O$, 0.1 mol/L) was dissolved in a anhydrous ethanol solution at room temperature as the precursor. Then, clean FTO/glass substrates were dipped into the precursor, withdrawn at 0.2 cm/s and dried in the air. The above dip-coating was repeated ten times. Finally, the as-coated substrates were heated in the air at a rate of 2 °C/min up to 500 °C and held at 500 °C for 60 min to obtain dense and transparent ZnO seed layer on FTO/glass substrates.

Preparation of ZnO nanorod arrays

A typical method for synthesizing the ZnO nanorod array film was carried out as in the literature [29]. In short, the well-aligned ZnO nanorod array film on ZnO-coated substrates was prepared from hydrothermal treatment in a Teflon-lined stainless autoclave. The precursor aqueous solution for the growth of ZnO nanorod arrays were prepared in advance by mixing $Zn(NO_3)_2{\cdot}4H_2O$ (HMT, 0.025 mol L^{-1}) and $(CH_2)_6N_4$ (0.025 mol L^{-1}) keeping their volume ratio at 1:1 in deionized water with stirring at ice-bathing condition. Then, the ZnO seed layer substrate was immersed into the precursor solutions at 95 °C in Teflon-lined stainless autoclave for 7 h without any stirring. Subsequently, the resultant film was thoroughly washed with deionized water and then heated at 500 °C for 1 h in the air.

Deposition of CdS on ZnO nanorod array film by chemical bathing deposition

The ZnO/CdS nanorod array film was prepared by depositing of CdS on ZnO nanorod arrays via chemical bathing deposition. The ZnO nanorod array film was immersed into the clear reactant solution containing cadmium nitrate ($Cd(NO_3)_2$, 0.01 M) and thioacetamide (C_2H_5NS, 0.01 M) at room temperature for 15 min. CdS growth was observed by the emergence of a yellow color on the sample surface. The modified film was thoroughly washed by deionized water in order to remove the surface residue and finally dried in the air. After the treatment, the samples were annealed again at 350 °C in N_2 atmosphere for 60 min.

Deposition of TiO_2 layer on ZnO/CdS nanorod array film by vacuum dip-coating process

The TiO_2 layer on ZnO/CdS nanorod array film (ZnO/CdS/TiO_2) was prepared by vacuum dip-coating process. Precursor solutions for TiO_2 layer were prepared according to

the process in the literature [30]. In a vacuum condition, the substrate was immersed into the TiO_2 precursor solutions. And then the samples were dried at 100 °C for 20 min. Finally, the samples were heat-treated at 450 °C for 30 min.

Materials characterization

The morphology of the films were inspected using a field emission scanning electron microscope (FESEM, Hitachi S-4800) equipped with a detector for energy dispersive spectroscopy (EDS).

Transmission electron microscope (TEM) was carried out using a JEM-1010 microscope with an acceleration voltage of 100 kV. For the TiO_2 layer on ZnO/CdS nanorod array film, the powder sample was scratched off the FTO substrate and then dispersed in the absolute ethyl alcohol.

The crystalline phase of the films were investigated with x-ray diffraction (XRD, X'Pert-PRO, PANalytical, Holland) equipped with Cu Kα radiation ($\lambda = 0.154056$ nm) at an accelerating voltage of 40 kV and a current of 40 mA. The patterns were recorded in the 2θ range from 20° to 80° at a scan rate of 1.5°/min.

The diffuse reflectance spectra (DRS) of films were recorded by a UV–Vis spectrophotometer (LAMBDA 750) equipped with an integrating sphere and with $BaSO_4$ as a reference in the range of 300–700 nm. The width of slit was 2.0 nm and the step was 0.5 nm.

Characterization of PEC behaviors and photoeletrocatalytic activity

All PEC tests were performed in a three-electrode electrochemical cell with a quartz window under the illumination of a 300 W xenon lamp (with a visible band pass filter glass, 390–770 nm) at room temperature. Transient photocurrent (i_{ph}) and linear sweep voltammetry (LSV) were employed in the three-electrode system, which was linked with CHI660A electrochemical station (CH Instruments, USA). A ZnO thin film electrode, a platinum sheet and a saturated calomel electrode (SCE) served as working electrode, counter electrode and reference electrode, respectively. The working electrode was mounted in a special holder with an area of 0.07 cm^2 exposed to a quartz window for visible light illumination. A 0.10 M $NaNO_3$ supporting electrolyte solution was chosen as the supporting electrolyte throughout all the experiments.

The photoelectrocatalytic activity was evaluated through the photoelectrocatalytic degradation of MB in the three-electrode system with an area of 7.5 cm^2 exposed to a quartz window for visible light illumination. The volume of the reactor was 75 mL, where the initial concentration of MB was 5×10^{-6} M. The MB solutions were taken out to collect their UV–Vis absorbance data once every 10 min. The photocatalytic or photoelectrocatalytic degradation of MB has been investigated under visible light illumination in the following conditions: (1) without photocatalyst, (2) pure ZnO nanorod arrays and Pt sheet used as working electrode by applying a bias of 0.2 V, (3) with the ZnO/CdS/TiO_2 used as working electrode without bias, (4) with the ZnO/CdS or ZnO/CdS/TiO_2 used as working electrode by applying a bias of 0.2 V.

Results and discussion

Morphologies and structures

Figure 2a, b, and c show the typical FESEM images of ZnO, ZnO/CdS and ZnO/CdS/TiO_2 nanorod array film on the ZnO-coated FTO glass substrate, respectively. Figure 2a shows the typical FESEM images of ZnO nanorod array film on the ZnO-coated FTO glass substrate. It can be clearly observed from Fig. 2a that highly dense ZnO nanorods with hexagonal structure and a rather smooth surface have grown on the FTO substrate. The cross-section image shows that the diameter of the ZnO nanorods is in the range from 100 to 150 nm and the length is approximately 2 μm. After chemical bathing deposition, the nanorods retain their hexagonal geometry, as shown in Fig. 2b. Compared with ZnO nanorods in the Fig. 2a, the nanorods exhibit an increase in approximately 20 nm in diameter and the surface of nanorod becomes roughened. These illuminate that nanoscale CdS coating is densely packed on the ZnO nanorod. The FESEM image of CdS-sensitized ZnO nanorod after coating with TiO_2 layer is shown in Fig. 2c. Figure 2d shows the TEM of CdS/ZnO/TiO_2 nanorod indicating that CdS-sensitized ZnO nanorods are uniformly and compactly coated by $\sim$5 nm thick TiO_2 layer.

The elemental composition was further analyzed by EDS, as shown in Fig 2e. The M_α peak of Cd and S can be seen clearly at 2.8 and 2.35 keV, respectively. Besides the strong K_α and K_β peaks of Zn element appear at 1.0 and 8.65 keV, a moderate K_α peak of the element O can also be observed at 0.52 keV. A moderate K_α peak of the element Ti can be observed at 0.4, 4.65, and 4.95 keV. Moreover, quantitative analysis of the EDS spectrum reveals that the molar ratio of Cd to S is close to 1:1, further confirming the stoichiometric formation of CdS. The quantification of the proportion of TiO_2 in the heterostructure is about 1.76% (atomic ratio).

Figure 3 shows the XRD patterns of FTO substrate (a), the pure ZnO nanorods (b), ZnO/CdS (c), and ZnO/CdS/TiO_2 (d), respectively. ZnO with a hexagonal crystalline structure reported in JCPDS card (No. 36-1451) are all shown in Fig. 3b–d. A strong peak at $2\theta = 34.4°$ is corresponded to the ZnO (002) crystal plane, which is further confirmed by the oriented ZnO nanorod arrays with preferential growth in

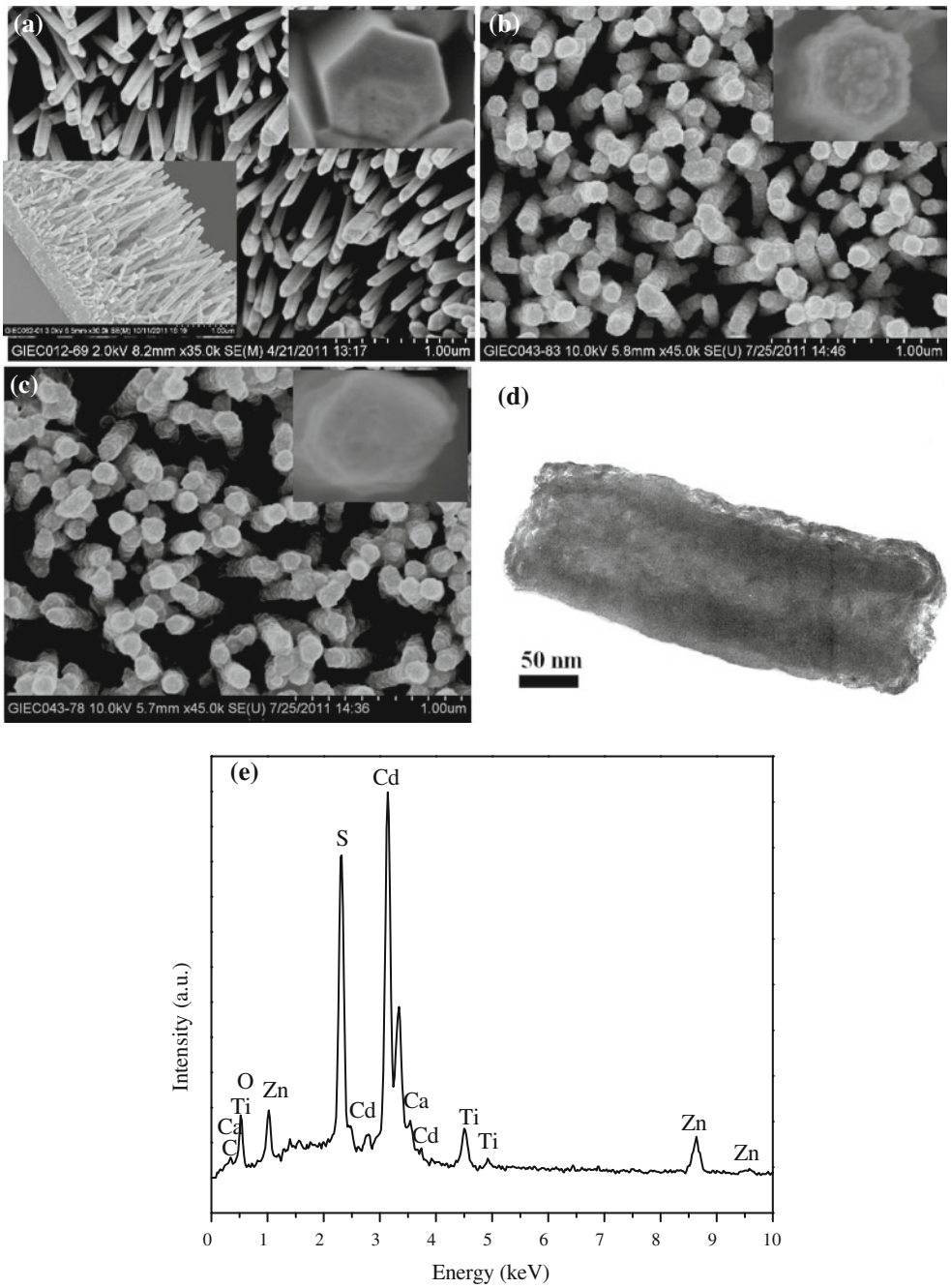

Fig. 2 FESEM images of ZnO nanorod arrays (**a**), ZnO/CdS (**b**), ZnO/CdS/TiO_2 (**c**); TEM image of ZnO/CdS/TiO_2 (**d**), and EDS spectrum of ZnO/CdS/TiO_2 (**e**)

the c-axis orientation. After the ZnO nanorod arrays were subject to the chemical bathing deposition process, some additional diffraction peaks corresponding to the hexagonally structured CdS phase (JCPDS Card No. 41-1049) appear at $2\theta = 24.8°$, 27.6°, and 44.1°, revealing that hexagonally structured CdS is produced. In Figure. 3d, the peak at $2\theta = 25.4°$ widening compared with Fig. 3c and a new diffraction peak appeared at 68.15° can be deduced the existence of TiO_2.

UV–Vis diffuse reflectance spectra

Figure 4 shows UV–Vis diffuse reflection spectra (DRS) of ZnO nanorods, ZnO/CdS and ZnO/CdS/TiO_2. The pure ZnO nanorod array film has no remarkable absorption of visible light with a wavelength above 400 nm (Fig. 4a), whereas the ZnO/CdS film extends the absorption spectrum obviously into the visible region (Fig. 4b). The UV–Vis absorption edge is relevant to the energy band of semiconductor. It can

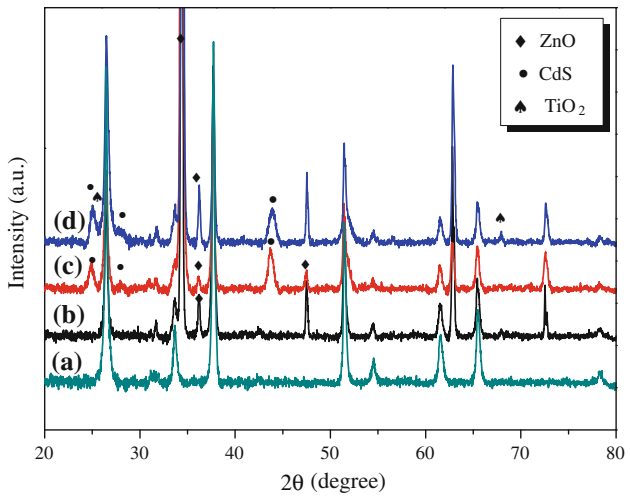

Fig. 3 XRD patterns of FTO substrate (**a**), ZnO nanorod arrays (**b**), ZnO/CdS (**c**), and ZnO/CdS/TiO_2 (**d**)

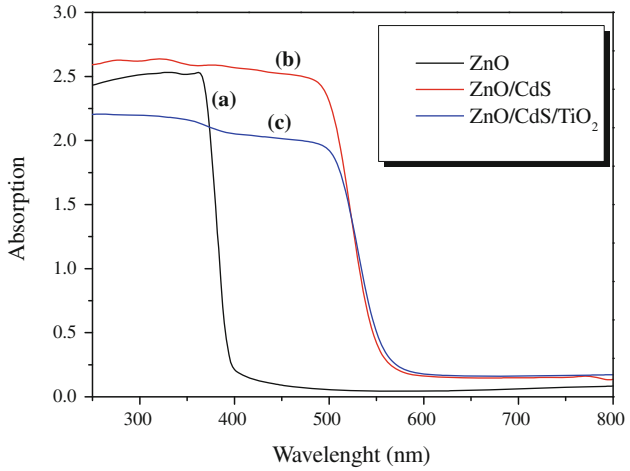

Fig. 4 UV–Vis absorption spectra of ZnO nanorod arrays (**a**), ZnO/CdS (**b**), and ZnO/CdS/TiO_2 (**c**)

be seen from Fig. 4 that the ZnO/CdS film shows an absorption edge at ~560 nm, corresponding to the energy band gap about 2.24 eV and which are bigger than that of bulk CdS (2.1 eV). The results provide the proof of size quantization effects of CdS nanocrystallites of ZnO/CdS nanorod array. After being coated by TiO_2 layer, there is almost no change in the absorption region, but the intensity of absorption decrease in the range from 300 to 500 nm.

The PEC behaviors

Linear sweeping voltammetry (LSV) and transient photocurrent (i_{ph}) were be used to investigate the PEC behaviors of the ZnO thin film electrode.

LSV can be applied to investigate the redox performance of semi-conductive films. LSV voltammograms of ZnO, ZnO/CdS, and ZnO/CdS/TiO_2 electrodes were measured

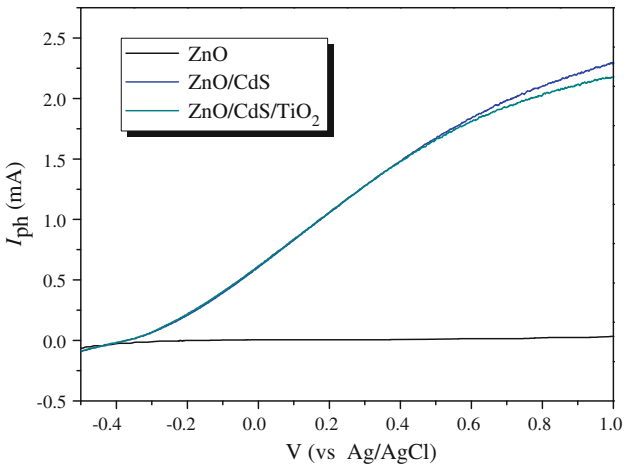

Fig. 5 LSV plots of the ZnO nanorod array, ZnO/CdS and ZnO/CdS/TiO_2 films under visible light illumination

under visible illumination at a scan rate of 10 mV/s. As shown in Fig. 5, no evident photocurrent for ZnO electrode is tested, which suggests that no typical electrochemical oxidation of water in the surface of ZnO electrode. The photocurrents of ZnO/CdS and ZnO/CdS/TiO_2 electrodes increase sharply with the increasing of bias potential and reached nearly 2.2 and 2.26 mA at 1.0 V, respectively. The anodic photocurrent of ZnO/CdS or ZnO/CdS/TiO_2 electrode is much higher than that of ZnO nanorod array film under visible illumination, which reveals that a larger number of photogenerated electrons flow to the cathode through the external circuit and the photogenerated holes leave in the photoelectrode for photocatalytic oxidation.

Transient photocurrent (i_{ph}) is generated from the photoelectrons excited from the semi-conductive valance band to the conducting band. The transient photocurrent of ZnO/CdS or ZnO/CdS/TiO_2 electrode was measured at a fixed bias potential of 0.2 V versus SCE with a visible light pulse of 20 s. Fig. 6 shows the comparison of transient photocurrent between the ZnO/CdS electrode and the ZnO/CdS/TiO_2 electrode. At the preliminary stage of illustration, the i_{ph} of ZnO/CdS electrode is larger than that of ZnO/CdS/TiO_2 electrode. Subsequently, the i_{ph} of ZnO/CdS electrode decays gradually with the increasing of the on/off cycles illustration. At the late stage of illustration, it is even lower than that of ZnO/CdS/TiO_2 electrode. However, ZnO/CdS/TiO_2 electrode exhibits the stability of photocurrent. This result indicated that the TiO_2 layer on the ZnO/CdS as a stable shell can effectively protect the CdS from photocorrosion.

The photoelectrocatalytic activity

Figure 7a shows the concentration changes of MB without photocatalyst and over Pt sheet or pure ZnO nanorod array film electrode by applying a bias of 0.2 V under the

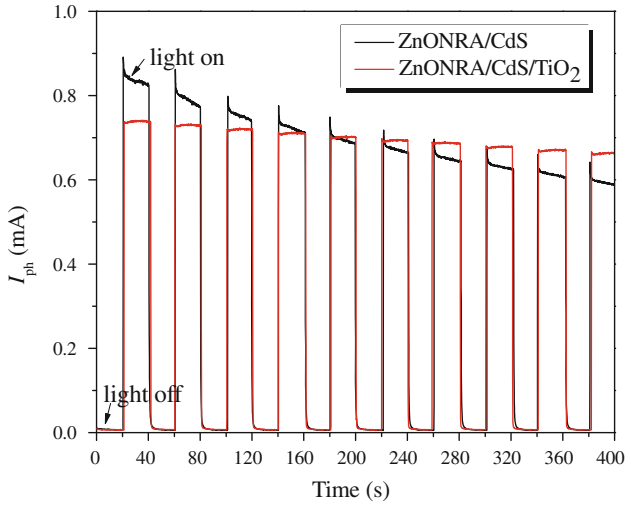

Fig. 6 Photocurrents of ZnO/CdS and ZnO/CdS/TiO_2 under visible illumination

irradiation of visible light. It could be seen that they can only results in about 8.9% MB degradation ratio after 90 min. For ZnO/CdS/TiO_2 used as photocatalyst, there is a rapid degradation of MB with 85.8% MB degradation ratio after 90 min. A higher efficiency for MB degradation can be further achieved by applying a bias of 0.2 V.

Figure 7b shows the photoelectrocatalytic activity of ZnO/CdS and ZnO/CdS/TiO_2 films at different batches by applying a bias of 0.2 V under the irradiation of visible light. For the first run, MB degradation ratio for ZnO/CdS electrode was slightly larger than that of ZnO/CdS/TiO_2 electrode at the preliminary stage. At the late stage, it is even lower than that of ZnO/CdS/TiO_2 electrode. MB degradation ratio achieves to 88.1% after 90 min by ZnO/CdS, which is lower than 91.3% for ZnO/CdS/TiO_2. These results are consistent with the photocurrents of ZnO/CdS electrode and ZnO/CdS/TiO_2 electrode (Fig. 6). To examine the photocatalytic stability of the ZnO/CdS and ZnO/CdS/TiO_2, the used ZnO/CdS and ZnO/CdS/TiO_2 photocatalysts were employed to degrade MB under visible light for five times. The experiment results of the five beaches are shown in the inset of Fig. 7b (up for ZnO/CdS, below for ZnO/CdS/TiO_2). The decay of photocatalytic activity for ZnO/CdS is rapidly. The degradation ratio of MB at 90 min decreases to 47.3% in the five run. However, it is found that there is no remarkable difference between the five repeated batches for ZnO/CdS/TiO_2 photoelectrocatalytic degradation of MB. These results indicate that the photocatalytic activity of ZnO/CdS/TiO_2 is stable.

For CdS-sensized ZnO nanorod array film, when CdS is illuminated by visible light, the photoelectrons would be excited from the valance band to the conducting band and then the photoelectrons are injected into the lower ZnO conducting band. The injected electrons could be

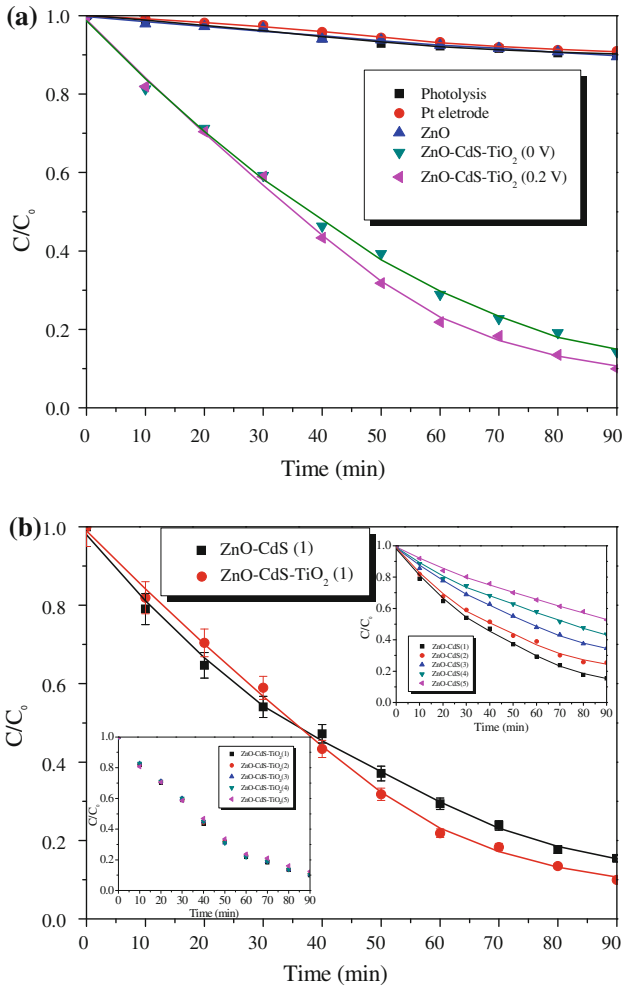

Fig. 7 Photoelectrocatalysis degradation of MB over ZnO/CdS and ZnO/CdS/TiO_2 electrodes

propitious to transfer from the vertical-aligned ZnO nanorod arrays to the cathode. Owing to the effective charge separation, the rate of hole-electron recombination in CdS is suppressed. Thus, the light conversion efficiency is enhanced effectively. In the photocatalytic oxidation reaction, TiO_2 layer provide an efficient channel for the photogenerated holes from CdS surface to heterosystem/electrolyte boundary [31]. The holes at the boundary can react with water to give the OH radicals, which subsequently attack the organic compound, such as MB. By introducing a TiO_2 layer to prevent CdS photocorrosion, the CdS-sensized ZnO nanorod array film could be used as a potential visible light photocatalyst.

Conclusions

In summary, we report a novel ZnO/CdS/TiO_2 nanorod array composite structure which was fabricated by

depositing CdS-sensitized layer onto ZnO nanorod arrays via chemical bathing deposition and subsequently coated by TiO_2 protection layer via a vacuum dip-coating process. The ZnO/CdS/TiO_2 nanorod array film possesses stable and superior photoelectrocatalytic performance under visible light irradiation owing to the TiO_2 thin layer protecting the CdS from photocorrosion.

Acknowledgement The study is supported by the National Natural Science Foundation of China (No. 51172233), the Science & Technology Plan Project of Guangdong Province (No. 2009B030400002) and National 973 project of China (No. 2009CB220002).

References

1. Doerffler W, Hauffe K (1964) J Catal 3:156
2. Yamagata S, Loo BH, Fujishima A (1989) J Electroanal Chem 260:447
3. Linsebigler AL, Lu GQ, Yates JT (1995) Chem Rev 95:735
4. Wu YS, Wei HY, Lun N, Zhao F (2004) J Mater Sci 39:1305. doi: 10.1023/B:JMSC.0000013889.63705.f3
5. Lee GW, Choi SM (2008) J Mater Sci 43:715. doi:10.1007/s10853-007-2200-y
6. Zhang YY, Li XJ, Chen JZ (2010) Catal Lett 139:129
7. Jia HM, Xu H, Hu Y, Tang YW, Zhang LZ (2007) Electrochem Commun 9:354
8. Sun WT, Yu Y, Pan HY, Gao XF, Chen Q, Peng LM (2008) J Am Chem Soc 130:1124
9. Tak Y, Kim H, Lee D, Yong K (2008) Chem Commun 38:4585
10. Sun YP, Hao E, Zhang X, Yang B, Shen JC, Chi LF, Fuchs H (1997) Langmuir 13:5168
11. Sung YM, Lee JC, Kim TG, Choi HJ (2007) Appl Phys Lett 91:113104
12. Tiefenbacher S, Pettenkofer C, Jaegermann W (1984) J Appl Phys 91:2002
13. Kang YS, Sudhagar P, Jung JH, Park S, Sathyamoorthy R, Ahn H (2009) Electrochim Acta 55:113
14. Lee YL, Chi CF, Weng HS (2008) Nanotechnology 19:125704
15. Tak Y, Hong SJ, Lee JS, Yong K (2009) J Mater Chem 19:5945
16. Wang LD, Ma BB, Luo F, Wu XM, Zhan C, Qiu Y (2007) Jpn J Appl Phys 46:7745
17. Parkinson BA, Sambur JB, Riha SC, Choi D (2010) Langmuir 26:4839
18. Houskova V, Stengl V, Bakardjieva S, Murafa N (2008) J Phys Chem Solids 69:1623
19. Karunakaran C, Abiramasundari G, Gomathisankar P, Manikandan G, Anandi V (2011) Mater Res Bull 46:1586
20. Xi GC, Ouyang SX, Ye JH (2011) Chem Eur J 33:9057
21. Sartori A, Visentin F, Habra NE, Zorzi CD, Natali M, Garoli D, Gerbasi R, Casarin M, Rossetto G (2011) Cryst Res Technol 46:885
22. Ku Y, Huang YH, Chou YC (2011) J Mol Catal A 342:18
23. Robert D, Bessekhouad Y, Chaoui N, Trzpit M, Ghazzal N, Weber JV (2006) J Photochem Photobiol A 183:218
24. Yu JC, Ho WK (2006) J Mole Catal A 247:268
25. Zhang JC, Li Q, Cao WL (2003) Chin J Catal 24:831
26. Zhao GH, Zhang YN, Lei YZ, Wu ZY, Jin YN, Li MF (2010) Mater Lett 64:2194
27. Raychaudhuri AK, Chander R (2006) J Mater Sci 41:3623. doi: 10.1007/s10853-006-6218-3
28. Zhou FL, Li XJ, Shu J, Wang J (2011) J Photochem Photobiol A 219:132
29. Cai ZS, Xu B (2008) Appl Surf Sci 254:5899
30. Pecchi G, Reyes P, Sanhueza P, Villasenor J (2001) Chemosphere 43:141
31. Suleymanov MS (1991) Int J Hydrogen Energy 16:741